butane in the aqueous solution.[17] The decrease of the effective attractive monomer-monomer interaction occurs because the addition of urea increases the static dielectric constant of the aqueous solution. And the increase in γ may be due to the fact that some urea molecules are attached to the hydrophilic part of the PC molecule and thus increase its effective molecular volume in water. More definitive statements on these points can be made after analysis of small-angle neutron scattering experiments which we are presently undertaking.

Acknowledgment. B.L.C. is grateful for the continued support of an Exxon Graduate Fellowship and in particular to Dr. J. S. Huang for his interest and advice during the course of this project. G.B. acknowledges partial support from Eniricerche (Italy). We appreciate the assistance of John Chen and Jack Cheng in the measurement of some of the cloud points. This research is supported by an N.S.F. grant administered by the Center for Materials Science and Engineering at M.I.T.

(17) Wetlaufer, D. B.; Malik, S. K.; Stoller, L.; Coffin, R. L. *J. Am. Chem. Soc.* **1964**, *86*, 508.

Rapid Cleavage Reactions of Haloaromatic Radical Anions Measured with Fast-Scan Cyclic Voltammetry

David O. Wipf and R. Mark Wightman*

Department of Chemistry, Indiana University, Bloomington, Indiana 47405 *(Received: December 15, 1988)*

Cyclic voltammetry at scan rates from 10 mV/s to 10^6 V/s has been used to characterize the reduction of aryl and benzyl halides in acetonitrile solutions containing 0.6 M tetraethylammonium perchlorate. The use of very rapid scan rates is made possible with electrodes of micrometer dimensions. The kinetics and mechanism of the reduction process have been evaluated by digital simulation of the recorded voltammograms. The radical anion generated at the electrode surface is found to have a half-life ranging from less than 100 ns in the case of 4′-bromoacetophenone to 70 ms for the case of *m*-nitrobenzyl chloride. The reduction mechanism for the aryl halides is consistent with the ECE–DISP1 mechanism. Thus, following initial one-electron reduction, halogen bond cleavage occurs resulting in a radical that is subsequently reduced. For the compounds with relatively long half-lives (>1 ms) the results in this work are in good agreement with prior investigations with cyclic voltammetry. Good agreement is also obtained with compounds that have a short half-life ($\sim$1 μs) which have been characterized by the technique of redox catalysis. However, the measured rate constants differ with previously reported values which were estimated or measured at the extreme time limits of classical electrochemical techniques.

Introduction

Cyclic voltammetry has often been used as a method to explore mechanisms of electrochemical oxidations or reductions. Classical cyclic voltammetry can be used to monitor electrogenerated transient compounds formed for times from tens of seconds to the submillisecond domain. The technique of redox catalysis developed by Saveant and co-workers has greatly extended the range of time scales available to voltammetric measurements.[1,2] However, recent developments in the miniaturization of electrodes and experimental procedure have led to a significant increase in the time resolution of cyclic voltammetry. Voltammograms with interpretable data have been obtained at the submicrosecond time scale with the use of scan rates in the millions of volts per second range.[3-7] Cyclic voltammetry, therefore, can now be used to directly monitor reactions over a time scale of 8 orders of magnitude.

This paper describes an investigation of the rate of halide cleavage in aryl and benzyl halide radical anions with the use of these new cyclic voltammetric methods. The one-electron reduction of alkyl and aryl halides has been of considerable interest to further characterize concerted and sequential electron-transfer/chemical reactions.[8-10] The general picture which has emerged is that alkyl halides are reduced with a simultaneous carbon–halogen cleavage. In contrast, aryl halides follow a sequential route, in which bond cleavage follows electron transfer. Cyclic voltammetry and redox catalysis have both been used to probe these mechanisms; however, the time resolution of cyclic voltammetry has prohibited the direct observation of very fast processes.

The established scheme for the reduction of many aryl halides in organic solvents is given by reactions 1 and 2.[10,11] Upon

$$\mathrm{ArX} + 1e^- \underset{}{\overset{k_1^\circ}{\rightleftharpoons}} \mathrm{ArX}^{\bullet -} \qquad E_1^\circ \tag{1}$$

$$\mathrm{ArX}^{\bullet -} \xrightarrow{k_1} \mathrm{Ar}^\bullet + \mathrm{X}^- \tag{2}$$

reduction, the aryl halide forms a radical anion which decays via cleavage to form a neutral radical and a halide anion (1) and (2). The aryl radical formed in this way has, in general, a much more positive reduction potential than the parent and can undergo further reduction either at the electrode surface (3) or by a homogeneous disproportionation reaction (4).

$$\mathrm{Ar}^\bullet + 1e^- \rightleftharpoons \mathrm{Ar}^- \qquad E_2^\circ \tag{3}$$

$$\mathrm{Ar}^\bullet + \mathrm{ArX}^{\bullet -} \underset{}{\overset{K_1}{\rightleftharpoons}} \mathrm{Ar}^- + \mathrm{ArX} \tag{4}$$

Reactions 1, 2, and 3 comprise an ECE mechanism, while reaction pathway 1, 2, and 4 is known as DISP1.[12] The aryl anion is a

(1) Saveant, J.-M.; Su, K. B. *J. Electroanal. Chem.* **1985**, *196*, 1-22.
(2) Andrieux, C. P.; Saveant, J.-M. *J. Electroanal. Chem.* **1986**, *205*, 43-58.
(3) Wipf, D. O.; Wightman, R. M. *Anal. Chem.* **1988**, *60*, 2460-2464.
(4) Wipf, D. O.; Kristensen, E. W. K.; Deakin, M. R.; Wightman, R. M. *Anal. Chem.* **1988**, *60*, 306-310.
(5) Andrieux, C. P.; Garreau, D.; Hapiot, P.; Saveant, J.-M. *J. Electroanal. Chem.* **1988**, *248*, 447-450.
(6) Andrieux, C. P.; Garreau, D.; Hapiot, P.; Pinson, J.; Saveant, J.-M. *J. Electroanal. Chem.* **1988**, *243*, 321-335.
(7) Amatore, C. A.; Jutand, A.; Pfluger, F. *J. Electroanal. Chem.* **1987**, *218*, 361-365.
(8) Newcomb, M.; Curran, D. P. *Acc. Chem. Res.* **1988**, *21*, 206-214.
(9) Andrieux, C. P.; Saveant, J.-M.; Su, K. B. *J. Phys. Chem.* **1986**, *90*, 3815-3823.
(10) Hawley, M. D. In *Encyclopedia of Electrochemistry of the Elements, Organic Section*; Bard, A. J., Lund, H., Eds.; Dekker: New York, 1980; Vol. XIV.
(11) M'Halla, F.; Pinson, J.; Saveant, J.-M. *J. Electroanal. Chem.* **1978**, *89*, 347-361.

* To whom correspondence should be addressed.

0022-3654/89/2093-4286$01.50/0

TABLE I: Experimental Results for the Reduction of Aryl Halides

no.	name	k_1, s^{-1}	k_1^0, cm s^{-1}	D, cm^2 s^{-1}	E_1^0, V	E_3^0, V	K_2
1	*p*-Br-benzophenone	4×10^4	2.4	1.1×10^5	−1.79	−1.88	3.3×10^1
2	9-Cl-anthracene	2×10^2	3.0	1.1×10^5	−1.78	−2.00	5.2×10^3
3	9-Br-anthracene	6×10^5	10	1.3×10^5	−1.76	−2.00	1.1×10^4
4	2-Cl-quinoline[a]	6×10^5	10	1.8×10^5	−1.93	−2.10	7.5×10^2
5	2′-Cl-acetophenone	3×10^5	1.3	1.4×10^5	−1.92	−2.01	3.3×10^1
6	4′-Cl-acetophenone	3×10^3	1.0	1.4×10^5	−1.91	−2.01	4.9×10^1
7	3′-Cl-acetophenone	15	1.0	1.4×10^5	−1.84	−2.01	
8	4′-Br-acetophenone	$>8 \times 10^6$[b]			>−2.08	−2.01	
9	3′-Br-acetophenone	8×10^3	1.0	1.0×10^5	−1.83	−2.01	1.1×10^3
10	*m*-nitrobenzyl Cl	10	0.25		−1.06	−1.17	
11	*p*-nitrobenzyl Cl	$>4 \times 10^6$[b]	~0.25			−1.17	
12	*m*-nitrobenzyl Br	$>4 \times 10^3$[b]				−1.18	

[a] From ref 3. [b] Estimate; see text.

strong base and will readily be protonated by the presence of acidic impurities or the solvent itself.

$$Ar^- + H^+ \xrightarrow{k_2} ArH \quad (5)$$

A third reduction pathway for the radical is also possible. The aryl radical can abstract a hydrogen atom from the solvent. The solvent radical formed in this way can be reduced at the electrode or in solution as outlined below. Reactions 1, 2, and 6 compose the hydrogen atom transfer (HAT) mechanism. If protons are readily available, the solvent anion will be protonated (9).

$$Ar^\bullet + SH \rightarrow ArH + S^\bullet \quad (6)$$

$$S^\bullet + 1e^- \rightleftarrows S^- \quad (7)$$

$$S^\bullet + ArX^{\bullet-} \rightleftarrows S^- + ArX \quad (8)$$

$$S^- + H^+ \rightarrow SH \quad (9)$$

This mechanism cannot be distinguished from reactions 1–5 by cyclic voltammetry if $S^\bullet$ is reduced more easily than $Ar^\bullet$.

The neutral aromatic compound formed by reaction 5 or 6 is usually reducible at more negative potentials than the parent aromatic halide compound (10). The presence of significant amounts of the aromatic radical anion will allow the occurrence of an additional solution reduction of the parent aromatic halide.

$$ArH + 1e^- \rightleftarrows ArH^{\bullet-} \qquad E_3^\circ \quad (10)$$

$$ArH^{\bullet-} + ArX \underset{K_2}{\rightleftharpoons} ArH + ArX^{\bullet-} \quad (11)$$

The ECE and DISP1 pathways lead to an overall two-electron reduction as observed at the electrode. When enough protons are present to protonate the solvent anion, the HAT mechanism will also lead to a two-electron reduction. The actual reduction pathway is a competition between the three processes, and conditions governing this competition have been evaluated.[13-15]

For aromatic halide compounds that form unstable radical anion intermediates, much of the experimental data are consistent with the above mechanisms, i.e., a two-electron irreversible reduction followed by a one-electron reduction of the unsubstituted aromatic compound. In a number of cases, however, the first reduction involves an overall electron transfer of between one and two electrons.[11,16-18] The apparent cause of this is a competitive set of pathways that involves the aromatic or solvent radical. For example, the radicals can dimerize. Alternatively, Saveant has shown that the anions of solvents such as acetonitrile and dimethyl sulfoxide are strong nucleophiles and can engage in nucleophilic substitution. These processes have been thoroughly discussed elsewhere.[11,16]

In this paper, we have used cyclic voltammetry in conjunction with simulation techniques to determine the cleavage rate constants and standard reduction potentials of the radical anions of a group of aromatic radical anions in acetonitrile. Many of these exhibit reaction rates that are too rapid to be evaluated with classical cyclic voltammetry. Rate constants in the range of 10^1–10^6 s^{-1} are reported. The values measured in this work will be compared, where possible, to values obtained indirectly—either by redox catalysis or by estimates based on long-time behavior. Comparison will also be made with a report that appeared during the preparation of this paper in which fast-scan cyclic voltammetry was used to examine two of the compounds reported here in another aprotic solvent, dimethylformamide.[19]

Results

Evaluation of Kinetic and Thermodynamic Parameters. Cyclic voltammetry was used to investigate the reduction of a series of aromatic halide compounds over a scan rate range of 10^{-2}–10^6 V/s. The data for the experimental and estimated electrochemical and kinetic parameters determined for the compounds studied are given in Table I. Results for the individual species investigated are given below.

The compounds investigated were evaluated according to a mixed ECE–DISP1 mechanism as outlined in the Introduction. Data that are inconsistent with the ECE–DISP1 mechanism are noted later in this paper. It is useful to describe the cyclic voltammetric response to the above mechanism by defining a dimensionless chemical parameter, $\lambda = k_1/(vnF/RT)$, where v is the scan rate in V/s, F is the Faraday constant, R is the gas constant, and T is temperature. When λ is large (>100) and the electron transfer is reversible, the observed cyclic voltammetric wave will be an irreversible, two-electron wave. Theoretically, the wave height will be 2.2 times the height of a wave unencumbered by chemical kinetics, i.e., $n_{app} = 2.2$.[12] Also, the peak position will shift by 30 mV for every 10-fold increase in λ. As the value of λ becomes smaller, n_{app} smoothly approaches a value of 1 as $\lambda \rightarrow 0$, and the shift in peak position approaches the chemically reversible, one-electron value. At the same time, the wave will begin to develop an appreciable reverse wave. Parts C and D of Figure 1 include graphs of the peak position and n_{app} with λ. Deviations from the theoretical behavior will occur with slow electron-transfer kinetics or if Ohmic drop is present. Nearly all cyclic voltammograms obtained at scan rates above 100 V/s will suffer from one or both of these effects.

An estimate of the value of the cleavage rate constant can be obtained by simulating the cyclic voltammetric response for experimental voltammograms obtained over a wide scan rate range. The simulations used in this work are based on the mechanism for reactions 1–6 and 11 and have been discussed in a previous

(12) Nadjo, L.; Saveant, J.-M. *J. Electroanal. Chem.* **1973**, *48*, 113–145.
(13) Amatore, C. A.; Pinson, J.; Saveant, J.-M.; Thiebault, A. *J. Am. Chem. Soc.* **1982**, *104*, 817–826.
(14) Saveant, J.-M. *Acc. Chem. Res.* **1980**, *13*, 323–329.
(15) M'Halla, F.; Pinson, J.; Saveant, J.-M. *J. Am. Chem. Soc.* **1980**, *102*, 4120–4127.
(16) Lawless, J. G.; Hawley, M. D. *J. Electroanal. Chem.* **1968**, *21*, 365–375.
(17) Lawless, J. G.; Bartak, D. E.; Hawley, M. D. *J. Am. Chem. Soc.* **1969**, *91*, 7121–7127.
(18) Gores, G. J.; Koeppe, C. E.; Bartak, D. E. *J. Org. Chem.* **1979**, *44*, 380–385.
(19) Andrieux, C. P.; Hapiot, P.; Saveant, J.-M. *J. Phys. Chem.* **1988**, *92*, 5987–5992.

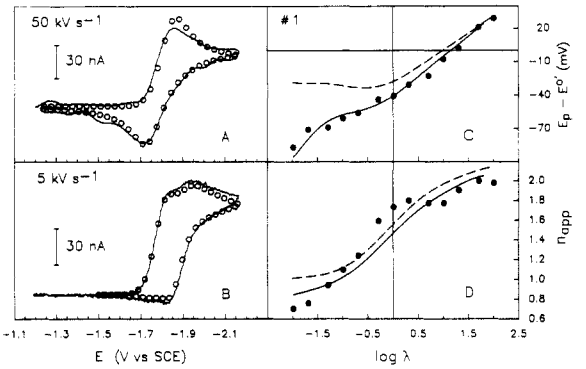

Figure 1. Reduction of 1.4 mM *p*-bromobenzophenone at 6- (A) and 10-μm-diameter (B) Au disk electrodes. (—) Background-subtracted cyclic voltammograms; (○) simulated cyclic voltammograms with parameters given in Table I. (C and D) (●) Plots of the experimental cyclic voltammetric peak position and n_{app} versus log λ; (- - -) theoretical behavior for the ECE–DISP1 mechanism (see text); (—) simulated behavior of the ECE–DISP1 mechanism for the experimental conditions given in the text and which also includes the effect of Ohmic drop and finite electron-transfer kinetics.

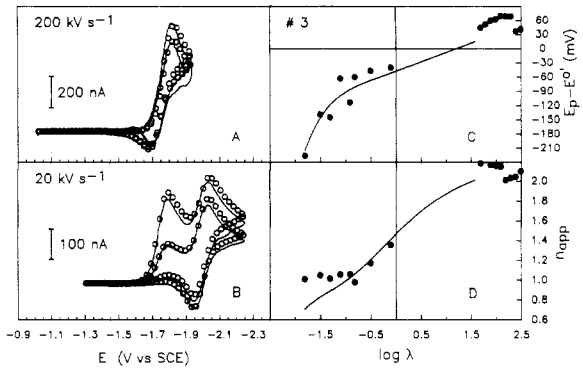

Figure 2. (A and B) Reduction of 4.8 mM 9-bromoanthracene at 6-μm-diameter Au disk electrodes. (—) Background-subtracted cyclic voltammograms with parameters given in Table I. (C and D) (●) Plots of the experimental cyclic voltammetric peak position and n_{app} versus log λ; (—) simulated behavior of the ECE–DISP1 mechanism for the experimental conditions given in the text and which also includes the effect of Ohmic drop and finite electron-transfer kinetics.

paper.[3] To model the first reduction wave, only reactions 1–4 need be considered. The simulation thus requires values for the formal reduction potentials, $E_1°'$ and $E_2°'$, the equilibrium constant K_1, and the cleavage rate constant, k_1. The value of $E_1°'$ is determined by the midpoint of the forward and reverse cyclic voltammetric peaks when the wave becomes reversible with respect to the chemical kinetics. The value of the reduction potential of the aryl radical ($E_2°'$) is not known but is likely positive of $E_1°'$ by 1 V or more.[20,21] The value of K_1 also requires knowledge of $E_2°'$ and can be calculated with

$$K_1 = \exp((nF/RT)(E_2°' - E_1°')) \qquad (12)$$

Fortunately, the effect of $E_2°'$ and K_1 on the first reduction wave are nearly constant once $E_2°'$ is more than a few hundred millivolts positive of $E_1°'$. A K_1 value of greater than 10^5 was used in all simulations. The diffusion coefficient, D, the heterogeneous rate constant, $k_1°$, and the electron-transfer coefficient, α, must be known as well. The diffusion coefficient can be estimated from the height of the two-electron wave seen at slow scan rates or by the one-electron reversible wave seen at fast scan rates. A value for $k_1°$ can be obtained from the separation of the forward and reverse waves of the chemically reversible voltammograms.[22] The transfer coefficient can usually be assumed to be 0.5.[23] Therefore, a simulation can be fit quite reasonably by adjustment of only simulation variable, λ.[25] The values used are given in Table I.

Simulations were performed for representative cyclic voltammograms encompassing the first wave. A visual best fit was obtained over a 10-fold range of scan rates by varying k_1. This procedure allowed assignment of a k_1 value with an error of less than 30%. To check the validity of the assigned rate constant, a series of simulations for a broad scan rate range (typically 4 orders of magnitude) were simulated for the first wave and the simulated and experimental n_{app} and peak position were plotted versus λ.

The second reduction wave and its return sweep wave can also be simulated to further test the fit to the assigned mechanism and simulation parameters. Additional terms must be included for the reduction potential of the second wave ($E_3°'$) and its associated heterogeneous kinetic parameters. Also, the second equilibrium constant K_2 must be used. It can be calculated in the same fashion as K_1. The pseudo-first-order rate constant k_2 is not known; however, this rate constant is probably diffusion controlled and therefore much faster than k_1.

p-Bromobenzophenone. The reduction of *p*-bromobenzophenone was investigated over a scan rate range of 20–100 000 V/s. At scan rates below 2000 V/s, the reduction process yields a chemically irreversible first wave followed closely by a second reversible wave. At faster scan rates the first wave becomes chemically reversible with the second wave diminishing. The response of the first wave for the variation in peak position and n_{app} was found to vary with scan rate in a manner consistent with a mixed ECE–DISP1-type reduction mechanism.

The experimental data for the variation of E_p as a function of scan rate fit well with the simulations for a k_1 value of 4×10^4 s^{-1} (Figure 1). The plot of n_{app} versus λ also shows good agreement with the exception of a small section of the curve near a λ value of 0. The experimental n_{app} in this region is larger than would be expected from simulations of the ECE–DISP1 mechanism for potential scans over the first wave. This is due to the overlap of the second reduction process with the first in this range of scan rates. When both reduction processes are accounted for, a good fit to the individual voltammograms is obtained (Figure 1).

9-Chloroanthracene. The reduction of 9-chloroanthracene for scan rates less than 10 V/s shows a chemically irreversible first wave followed by a reversible second wave. At greater scan rates the first wave becomes reversible and the second wave diminishes, consistent with an ECE–DISP1 process. A plot of E_p versus λ indicates a 29 mV per decade shift at scan rates less than 10 V/s and the apparent number of electrons smoothly changes from 2 to 1. Voltammograms that are chemically reversible are obtained at scan rates above 500 V/s. Simulations indicate that k_1 is 200 s^{-1}.

9-Bromoanthracene. The reduction of 9-bromoanthracene is similar to that seen for 9-chloroanthracene with the exception that the first wave is chemically irreversible at scan rates up to 100 000 V/s. At faster scan rates a reverse wave appears that is associated with the first wave. At these rapid scan rates Ohmic drop plays a large role in the shape of the voltammograms but can be accounted for in the simulation. Evaluation of the voltammetric data for the first wave yields a cleavage rate constant of 6×10^5 s^{-1} (Figure 2). The match between experiment and simulated cyclic voltammograms were not perfect for scan rates greater than 100 000 V/s, however. At these fast time scales the anodic to cathodic peak separation was less than obtained by the simulation. In addition, the peak currents at the fastest scan rates were larger than the simulated cyclic voltammograms. Similar behavior has also been reported for the reduction of 2-chloroquinoline,[3] a compound with a similar rate constant for the radical anion cleavage. Semiintegrals of the voltammograms at high scan rates

(20) Wayner, D. D. M.; McPhee, D. J.; Griller, D. *J. Am. Chem. Soc.* **1988**, *110*, 132–137.
(21) Juan, B.; Schwarz, J.; Breslow, R. *J. Am. Chem. Soc.* **1980**, *102*, 5741–5748.
(22) Nicholson, R. S. *Anal. Chem.* **1965**, *37*, 1351–1355.
(23) This assumption is consistent with measured values for the reduction of aromatic hydrocarbons.[24]
(24) Kojima, H.; Bard, A. J. *J. Am. Chem. Soc.* **1975**, *97*, 6317–6324.
(25) When systematic deviations in peak height were observed, $D^{1/2}$ was altered, but not by more than 10%. In a similar manner, systematic deviations in E_p were accounted for by adjustment of $k_1°$.

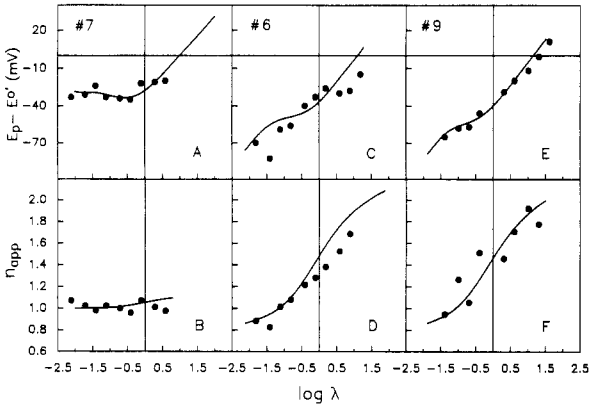

Figure 3. Plots of experimental and simulated cyclic voltammetric peak position and n_{app} for 3′-chloro- (**7**), 4′-chloro- (**6**), and 3′-bromoacetophenone (**9**). Simulation parameters are given in Table I. (O) experimental data; (—) simulation results with the EC mechanism for compound **7** and the ECE–DISP1 mechanism for compounds **6** and **9**.

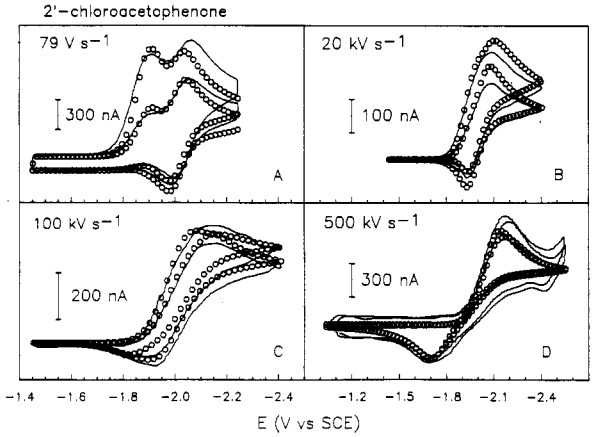

Figure 4. Reduction of 2′-chloroacetophenone. (—) Experimental cyclic voltammograms at concentrations of 0.77 (A) and 5.0 mM (B–D) at gold disk electrodes of 105- (A) and 6-μm diameter (B–D). Voltammograms B–D are background subtracted; (O) simulated cyclic voltammograms with parameters given in Table I and in the text.

met the criteria for diffusion control,[26] indicating that adsorption is not a significant contributor to the measured current.

3′-Chloroacetophenone. The reduction of 3′-chloroacetophenone at scan rates of less than 1 V/s consists of a one-electron chemically irreversible wave that becomes reversible at faster scan rates. The first wave is followed by a second, very small, reversible wave at slow scan rates. The behavior of the first wave, which shows complete chemical reversibility at scan rates greater than 40 V/s, suggests that the majority of the reduction process does not follow the ECE–DISP1 process, but instead follows EC behavior. Simulation of the cyclic voltammetric curves using an EC model (only reactions 1 and 2 operative) yields a value for k_1 of 15 s^{-1} (Figure 3).

4′-Chloroacetophenone. The reduction of 4′-chloroacetophenone at scan rates of less than 100 V/s indicate a chemically irreversible first wave followed by a reversible second wave. At faster scan rates the first wave exhibits a reverse wave. Complete chemical reversibility is observed at a scan rate of 5000 V/s. Simulations for the mixed ECE–DISP1 mechanism at scan rates larger than 100 V/s indicate that $k_1 = 3 \times 10^3$ s^{-1} (Figure 3). At scan rates below 100 V/s the simulation overestimates the height of the first wave. In addition, the experimental second wave is much smaller than the simulated value. This may indicate that the ECE–DISP1 mechanism is in competition with another mechanism that involves the aryl radical species.

2′-Chloroacetophenone. The reduction of 2′-chloroacetophenone at slow scan rates yields an irreversible first wave followed by a reversible second wave (Figure 4). As the scan rate approaches 20 000 V/s, the two waves merge into a single broad peak. The fusion of the initial and product waves makes analysis of the data difficult. However, simulations that take into account reactions 1–5, 10, and 11 can be used to analyze the data. At scan rates above 100 000 V/s the current contributed by the reducible product diminishes, and at 500 000 V/s the only apparent reduction process is that of the 2′-chloroacetophenone. Simulations indicate a k_1 value of 3×10^5 s^{-1}.

3′-Bromoacetophenone. The reduction of 3′-bromoacetophenone is very similar to that seen for 4′-chloroacetophenone. The major difference is that the measured current at slow scan rates is in better agreement with the ECE–DISP1 mechanism throughout the range of scan rates investigated. Complete chemical reversibility is observed as a scan rate of 5000 V/s. A good fit to the experimental data is observed for simulations incorporating a k_1 value of 8×10^3 s^{-1} (Figure 3).

4′-Bromoacetophenone. The reduction of 4′-bromoacetophenone consists of a two-electron, chemically irreversible wave followed by a reversible wave. At scan rates greater than 500 000 V/s the first wave merges with the second wave. No indication of chemical reversibility is observed for scan rates up to 10^6 V/s. Although a reduction in peak height due to Ohmic drop and heterogeneous kinetics occurs at rapid scan rates, no evidence of chemically reversible behavior is observed.

m-Nitrobenzyl Chloride. The first reduction wave for *m*-nitrobenzyl chloride is closely followed by a second smaller wave and is chemically irreversible up to scan rates of 1 V/s (Figure 5). Values of n_{app} plotted vs λ show good agreement with the ECE–DISP1 mechanism with n_{app} changing smoothly from 2 at slow scan rates to 1. Faster scan rates were used to evaluate the heterogeneous electron transfer rate constant. By consideration of the anodic and cathodic peak separation over a scan rate range of 50–800 V/s, a $k_1°$ value of 0.25 cm/s was obtained, which is considerably slower than for the compounds previously described (Table I). The value of $dE_p/d \log (v)$ at high sweep rate values was −30 mV, consistent with an electrode reaction limited by electron-transfer kinetics.

p-Nitrobenzyl Chloride. The reduction of *p*-nitrobenzyl chloride exhibits a chemically irreversible first wave, followed by a reversible wave at scan rates slower than 100 V/s (Figure 5). At scan rates larger than this and for concentrations greater than 1 mM, one irreversible wave is observed with a height that corresponds to a one-electron reduction. This wave shifts by −75 mV per decade scan rate as expected for simultaneous control by both chemical and electrochemical kinetics.[12] No indication of reversibility is seen for scan rates of up to 10^6 V/s. The relatively slow heterogeneous kinetics for the meta-substituted analogue lead to the expectation that electron transfer would be slow in this case as well.

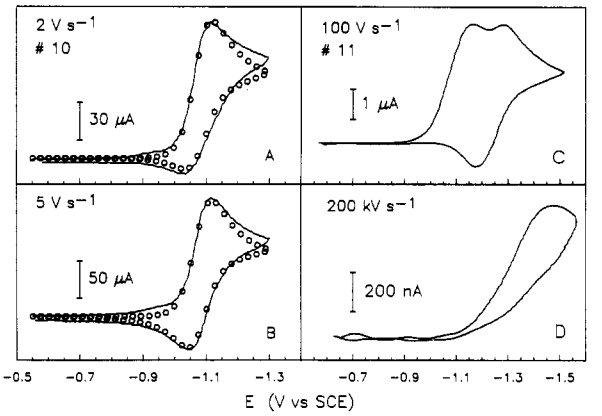

Figure 5. Reduction of *m*- and *p*-nitrobenzyl chloride. (A and B) (—) Cyclic voltammograms for 2.4 mM *m*-nitrobenzyl chloride at a 1.6-mm-diameter Au disk electrode; (O) simulations with parameters given in Table I. (C and D) (—) Cyclic voltammograms for 4.1 mM *p*-nitrobenzyl chloride at a (C) 105-μm-diameter Au disk and (D) 6-μm-diameter Au disk. Voltammograms C and D are background subtracted.

(26) Bowling, R.; McCreery, R. L. *Anal. Chem.* **1987**, *59*, 1615–1620.

TABLE II: Comparison of Experimental Values for the Cleavage Rate Constant

no.	name	k_1, s^{-1}	k_1(ref), s^{-1}	solvent	technique	ref
1	*p*-Br-benzophenone	4×10^4	2.4×10^3	CH_3CN	cyclic voltammetry	33
2	9-Cl-anthracene	2×10^2	2.6×10^2	CH_3CN	cyclic voltammetry	29
3	9-Br-anthracene	6×10^5	3.0×10^5	DMSO	redox catalysis	29
			1.5×10^5	CH_3CN	deuterium incorporation	15
			8.0×10^5	DMF	fast-scan cyclic voltammetry	19
4	2-Cl-quinoline	6×10^5	6.0×10^5	DMF	redox catalysis	29
6	4′-Cl-acetophenone	3×10^3	1.0×10^5	DMF	estimated	18
7	3′-Cl-acetophenone	15	5	DMF	chronoamperometry	18
9	3′-Br-acetophenone	8×10^3	6.0×10^4	DMF	fast-scan cyclic voltammetry	19
10	*m*-nitrobenzyl Cl	10	2.5	CH_3CN	chronoamperometry	17
11	*p*-nitrobenzyl Cl	$>4 \times 10^6$	2.0×10^4	CH_3CN	estimated	17
12	*m*-nitrobenzyl Br	$>4 \times 10^3$	3.5×10^1	CH_3CN	chronoamperometry	17

m-Nitrobenzyl Bromide. The reduction of *m*-nitrobenzyl bromide at slow scan rates is very similar to that observed for *p*-nitrobenzyl chloride. An initial, chemically irreversible reduction wave merges with a following reversible wave at scan rates larger than 10 V/s. The height of the first wave is consistent with one-electron transfer. No indication of reversibility is seen at scan rates of up to 1000 V/s. At scan rates larger than this the reduction is plagued by severe electrode fouling, evidenced by large reduction waves with characteristics of an adsorbed species, which occurred on both gold and platinum electrodes. This prohibited faster scan rates from being analyzed.

Discussion

The compiled experimental data (Table I) confirm several features previously recognized. The cleavage rate constants for the halide compounds with the same substrate decreases in the order of position on the aromatic ring in the series 2 > 4 > 3.[18,27,28] Brominated compounds have faster rate constants than the chlorinated analogues.[27,29] However, a plot of the reduction potential versus the rate constant for halide cleavage does not show a good correlation. In general, the rate of halide cleavage increases with a more negative reduction potential, a result predicted on theoretical grounds.[9] Several exceptions are seen, however. For example, 9-bromoanthracene is ~70 mV easier to reduce than 3′-bromoacetophenone and yet the rate of bond cleavage is ~100 times greater. A better correlation appears to exist among isomeric compounds (e.g., the chloroacetophenones).

Most of the aryl compounds examined fit the mechanism outlined in the Introduction well. Previous studies in which products have been identified after exhaustive electrolysis are consistent with these mechanisms.[10,15-18] Exceptions occur within the acetophenones. One explanation for the apparent one-electron reduction as is observed for 3′- and 4′-chloroacetophenone is that solvent anions formed via the HAT mechanism are available for nucleophilic attack. Nucleophilic substitution of the solvent anion has been shown to occur in the reduction of bromobenzophenone in dimethyl sulfoxide.[11] This product ($ArS^{\bullet -}$) may reduce the parent halide, resulting in a catalytic process.

$$Ar^{\bullet} + S^- \rightarrow ArS^{\bullet -}$$

$$ArS^{\bullet -} + ArX \rightarrow ArS + ArX^{\bullet -}$$

When this process is in competition with reactions 1–4, and ArS is electroinactive at the potential of ArX, an *n* value of less than 2 will be observed. However, ArS would be expected to be reduced at nearly the same potential as ArH. The lack of an appreciable wave for ArH after reduction of 3′-chloroacetophenone in acetonitrile suggests an alternate explanation. Bellamy has shown that electrogenerated $-CH_2CN$ adds readily to the carbonyl group on acetophenone and benzophenone.[30] Thus, an acetonitrile anion also could add to the chlorinated acetophenone to yield an alcohol that would be nonreducible in this potential range.

$$ArX + S^- \rightleftharpoons SArX$$

This mechanism would result in a lowering of both voltammetric waves. However, cyclic voltammetry alone cannot distinguish between either pathway. A third possibility is the formation of a dimer via radical coupling. However, Bartak reports that the reduction of 3′-chloroacetophenone in dimethylformamide gave no detectable amounts of the dimeric product.[18]

The reduction of 4′-chloroacetophenone also involves less than an overall transfer of two electron at potentials corresponding to the first wave at slow scan rates. This indicates that similar reduction pathways as with the 3′ analogue may be operating. In this case, these pathways leading to one-electron products are not as important, since, due to the faster cleavage rate constant, the aryl radical is formed much closer to the electrode where reaction 4 is more efficient. This is further evidenced by the 2′-chloro-, 4′-bromo-, and 3′-bromoacetophenones—all of which have faster cleavage rate constants than the 4′-chloro compound—having, at the lower scan rate limit, an n_{app} of 2.

The experimental data for the reduction of 4′-bromoacetophenone do not allow the assignment of a cleavage rate constant. However, an estimate of the lower limit of the anion radical cleavage rate constant can be made. For a compound with a cleavage rate constant of 8×10^6 s^{-1}, a 50% reduction of the peak height (i.e., $n_{app} = 1.6$) would occur at a scan rate of 200 000 V/s. Since this is not observed, the rate constant of 4′-bromoacetophenone must have a rate constant greater than 8×10^6 s^{-1}. The decomposition rate is sufficiently fast that the ECE pathway can dominate over DISP1 for this compound,[31] a situation not previously reported in electrochemical studies.

The nitrobenzyl halides show electrochemical behavior much different from the aryl halides. Although the peak height behavior for the reduction of *m*-nitrobenzyl chloride follows ECE–DISP1 behavior, we are not able to accurately simulate the exact shape of the individual voltammograms at scan rates less than 1 V/s. Thus, although we can report a value for the cleavage rate constant, the mechanism is not known. It has been shown that large-scale electrolysis leads to a one-electron reduction with nitrotoluene as an identified product.[17] Studies by ESR show that a variety of radicals are formed during electrochemical reduction whose distribution varies with initial concentration.[32] The possibility of multiple pathways precludes simulation of the voltammograms, except at fast scan rates where all of the chemical steps are outrun.

Estimates of the lower bounds of the cleavage rate constant for anion radicals of *p*-nitrobenzyl chloride and *m*-nitrobenzyl bromide can be made as well. Here, however, the slow electron-transfer kinetics, adsorption, and uncertainty over the exact reduction mechanism again precludes assignment of mechanism. For concentrations higher than 1 mM the reduction involves one electron, and in agreement with this, dimeric and polymeric

(27) Grimshaw, J.; Trocha-Grimshaw, J. *J. Electroanal. Chem.* **1974**, *56*, 443–446.
(28) Alwair, K.; Grimshaw, J. *J. Chem. Soc., Perkin Trans. 2* **1973**, 1150–1154.
(29) Andrieux, C. P.; Blocman, C.; Dumas-Bouchiat, J. M.; M'Halla, F.; Saveant, J.-M. *J. Am. Chem. Soc.* **1980**, *102*, 3806–3813.
(30) Bellamy, A. J.; Howat, G.; MacKirdy, I. S. *J. Chem. Soc., Perkin Trans. 2* **1978**, 786–793.
(31) Amatore, C. A.; Saveant, J.-M. *J. Electroanal. Chem.* **1978**, *86*, 227–232.
(32) Peterson, P.; Carpenter, A. K.; Nelson, R. F. *J. Electroanal. Chem.* **1970**, *27*, 1–9.

products have been reported. In these cases we have searched for an appreciable anodic peak current to determine the radical anion lifetime. An i_{pa}/i_{pc} ratio of 0.5 would occur at λ of 0.1 in the case of a reversible electron transfer for the EC and ECE cases. No reverse wave is observed for the reduction of *p*-nitrobenzyl chloride at scan rates of 100 000 V/s and higher, giving a lower bound for the rate constant of 4×10^6 s^{-1}. Likewise, for *m*-nitrobenzyl bromide, absence of a reverse wave at a scan rate of 1000 V/s gives a lower limit of 4×10^3 s^{-1} for the cleavage rate constant.

The rate constants measured in this work are compared with previous reports in Table II. For the slowest cleavage rates (compounds **2**, **7**, and **10**) where electrodes of conventional size were employed, the values agree well with previous measurements. The significant difference between our value and the literature report for *m*-nitrobenzyl bromide is likely because of a misinterpretation of the data in the original work. However, for the case of *p*-bromobenzophenone, which only exhibits complete chemical reversibility at scan rates greater than 10 000 V/s, an order of magnitude difference in measured rates is obtained. We consider our rate constant more reliable because conventional cyclic voltammetric procedures are at their upper limit in the measurement of such a fast reaction. Good agreement is found between our values and those obtained by redox catalysis (compounds **3** and **4**) despite the fact that the rates were measured in different solvents. Similarly, agreement is found with rapid cleavage rates with determined fast-scan cyclic voltammetry (compound **3**). Agreement is not so good for the more moderate rate of cleavage found with 3′-bromoacetophenone when compared in acetonitrile and dimethylformamide. However, in dimethylformamide the reduction mechanism differs from this work in that it is an overall one-electron process. Finally, it appears that estimates of cleavage rates from evaluation of substituent effects (Hammett-type plots) seem quite unreliable since our measured values are considerably different (compounds **6** and **11**).

Experimental Section

The experiments employed the flow-cell cyclic voltammetry design reported previously.[3,4,34] Briefly, this design allows the working electrode to be placed at the outlet of a flowing stream of supporting electrolyte. This stream can be quickly switched to a stream that also contains the reducible compound. This allows an accurate removal of the background from the faradaic current by acquiring voltammograms in both streams and subtracting the results. Full experimental details are given in ref 3.

Reagents. Tetraethylammonium perchlorate (TEAP; G. F. Smith Chemical Co., Columbus, OH) was recrystallized twice from hot, doubly distilled water and dried in vacuo at 60 °C prior to use. All other compounds were from Aldrich (Milwaukee, WI) with the exception of 9-chloroanthracene (Alfa Products, Danvers, MA) and were used as received. Acetonitrile (UV grade, <0.01% H_2O, Burdick & Jackson, Muskegon, MI) was used as received.

Voltammograms were recorded in acetonitrile with 0.6 M TEAP as supporting electrolyte. Solutions were sparged with argon prior to use.

Electrodes. Gold and platinum disk ultramicroelectrodes were prepared from microscopic wires (5-, 10-, and 100-μm nominal diameter, Goodfellow Metals, Cambridge, England) as described previously.[4,35] The diameters of the nominally 5- and 100-μm wire were found to be actually 6 and 105 μm, respectively, by electrochemical and electron micrographic measurements. A 1.6-mm-diameter gold electrode from BAS (West Lafayette, IN) was also used. Repeated polishing of the 1.6-mm-diameter gold electrode removed the polymer insulating material faster than the gold, leading to a degree of uncertainty regarding the actual area of this electrode. Voltammetry with the large electrode was performed in a conventional 25-mL cell.

For work requiring a three-electrode geometry a platinum coil served as a auxiliary electrode and an aqueous saturated sodium calomel electrode (SSCE) separated by a fine frit served as the reference. At fast scan rates or under two-electrode conditions a coil of silver wire served as a quasi-reference electrode.[36]

The size of the electrode used at a particular scan rate was governed by two criteria. The electrode was chosen so as to be small enough so that Ohmic drop was minimized, yet large enough so that semiinfinite linear diffusion conditions prevailed.

Instrumentation. Slow scan rates ($v < 50$ V/s) were obtained with the large electrode, and a locally constructed three-electrode potentiostat with provision for Ohmic drop compensation (via positive feedback) was used. At faster scan rates a two-electrode potentiostat was used with the smaller diameter electrodes.

Computer simulations of the cyclic voltammetric response were identical with those used previously and incorporated the relevant heterogeneous and homogeneous kinetic and thermodynamic values.[3] For simulations of the EC mechanism only reactions 1 and 2 were considered. The simulation procedure also accounts for the effect of Ohmic drop due to the faradaic and charging current.

Cyclic voltammograms shown in this paper have been, except where noted, subtracted from the background current. In addition, the cyclic voltammograms have been deconvoluted from the instrumental distortion when necessary (i.e., at scan rates > 20 000 V/s). All potentials are reported versus a saturated calomel electrode (SCE), except where noted. The SSCE and SCE potentials are equivalent at the level of precision reported here.

Conclusions

In summary, the data in this work extend the range of cleavage rates measured for organic halides. Furthermore, the data show that fast-scan cyclic voltammetry can be reliably used to measure submicrosecond half-lives. The chief limitations of the technique are slow electron-transfer kinetics for the parent compound or adsorption of the reactants or products. However, for the class of compounds examined here these limitations were not problematic in most cases. In this work the cyclic voltammetry technique is clearly demonstrated to be useful for the measurement of rate constants over 5 orders of magnitude.

Acknowledgment. This work was supported by a grant from the Chemical Analysis Division of the National Science Foundation. D.O'.W. gratefully acknowledges the support of a fellowship from the Monsanto Corporation.

Registry No. **1**, 90-90-4; **2**, 716-53-0; **3**, 1564-64-3; **4**, 612-62-4; **5**, 2142-68-9; **6**, 99-91-2; **7**, 99-02-5; **8**, 99-90-1; **9**, 2142-63-4; **10**, 619-23-8; **11**, 100-14-1; **12**, 3958-57-4; Au, 7440-57-5; acetonitrile, 75-05-8.

(33) Nadjo, L.; Saveant, J.-M. *J. Electroanal. Chem.* **1971**, *30*, 41–57.
(34) Howell, J. O.; Kuhr, W. G.; Ensman, R. E.; Wightman, R. M. *J. Electroanal. Chem.* **1986**, *209*, 77–90.
(35) Wightman, R. M.; Wipf, D. O. *Electroanalytical Chemistry*; Bard, A J., Ed.; Dekker: New York, 1988; Vol. 15.
(36) Sawyer, D. T.; Roberts, J. L. *Experimental Electrochemistry for Chemists*; Wiley: New York, 1974.